

Target optimization of a water-window liquid-jet laser–plasma source

J. de Groot, O. Hemberg,^{a)} A. Holmberg, and H. M. Hertz

Biomedical and X-Ray Physics, Royal Institute of Technology/Albanova, S-10691 Stockholm, Sweden

(Received 9 May 2003; accepted 27 June 2003)

We optimize the water-window x-ray flux and debris deposition for a liquid-jet laser plasma source by varying both the target diameter and the jet material. For two target liquids, methanol and ethanol, measurements of the $\lambda = 3.37$ nm C VI x-ray flux and the debris deposition rates are presented as function of the jet diameter. It is shown that the effective carbon debris deposition is more than 1 order of magnitude smaller for methanol, while the x-ray flux is reduced only $\sim 40\%$. The reduction in carbon debris deposition may be explained by reactive ion etching by oxygen from the plasma. Thus, the methanol water-window source may be operated at a $5\text{--}10\times$ higher flux without increasing the debris deposition. The optimization potentially allows a reduction of the exposure time of compact soft x-ray microscopy or other water-window applications based on such sources without increasing damage to sensitive x-ray optics. © 2003 American Institute of Physics. [DOI: 10.1063/1.1602571]

I. INTRODUCTION

Carbon-target laser plasmas are suitable compact soft x-ray sources for many water-window applications. Liquid-jet targets using ethanol have previously demonstrated long operating times and large reduction of debris compared to conventional target systems. In many applications it is important to maximize flux while minimize the debris deposition on x-ray optics. In the present article we investigate flux and debris as a function of target liquid and jet diameter and show that methanol jets of larger diameters significantly increase the flux while still keeping debris low.

Laser plasmas¹ are attractive compact soft x-ray sources due to their small size, high brightness, and high spatial stability. Regenerative targets based on liquid droplets^{2,3} or liquid jets^{4,5} provide fresh target material at high density for full-day operation without interrupts and it allows the use of high-repetition-rate lasers, thereby having potential for high average power. Furthermore, it reduces debris production several orders of magnitude compared to conventional targets⁶ and for certain liquids the debris deposition is practically eliminated.^{3,5} Thus, the effective photon flux may be increased a few orders of magnitude compared to conventional targets since collection optics may be used reasonably close to the plasma. By choosing a suitable target liquid and correct plasma conditions, the emission wavelength may be spectrally tailored to suit different applications, e.g., the extreme ultraviolet (EUV) (~ 0.1 keV, e.g., EUV lithography),^{7–9} soft x rays (~ 1 keV, e.g., microscopy and reflectometry),^{2,3,5,10} and hard x rays (~ 10 keV, e.g., diffraction).¹¹

Ethanol-based water-window liquid-jet laser–plasma sources have been used for compact subvisible-resolution x-ray microscopy^{12,13} and reflectometry¹⁴ and have potential for, e.g., x-ray photoelectron spectroscopy.¹⁵ This source is

dominated by the hydrogen and helium-like carbon emission at $\lambda = 3.37$ and 4.03 nm, respectively. The major source issues of importance for pursuing applications are the flux and/or brightness for short exposure times, the long-term damage of fragile x-ray optics by debris, and the stability and reliability for user friendliness. As regards the stability and reliability we have often chosen to operate the source in the liquid-jet mode as opposed to the droplet mode.⁴ Thereby the stability increases by avoiding fluctuations in the x-ray flux due to droplet drift.¹⁶ A nozzle fabrication method, based on glass capillaries,¹⁷ allows the operation of ethanol jets at higher pressure and larger jet diameters. This makes liquid jet operation possible without nozzle damage since the nozzle–plasma distance may be increased to several mm.

In the present article we focus on the flux and the long-term debris-induced damage to optics for carbon-emission water-window liquid-jet laser plasmas. Here the nozzles allow optimization of both target diameter and target liquid with respect to the laser pulse. Below quantitative measurements of the debris deposition at different direction from the plasma and the x-ray flux are presented for two different target liquids: methanol and ethanol. Somewhat surprisingly, the effective debris deposition rate is significantly lower for methanol than for ethanol. Thus, the x-ray flux can be significantly increased by increasing the methanol jet diameter without exceeding the current (ethanol) debris deposition rates.

II. EXPERIMENTAL ARRANGEMENT

A schematic arrangement of the liquid-jet laser–plasma x-ray source is shown in Fig. 1. The liquid jet is created by forcing ethanol or methanol through a capillary nozzle at a pressure of 100 bars resulting in a speed of >80 m/s. In the current experiments the jet diameter is varied between 10 and 50 μm . A 600 l/s turbo pump in combination with a cold trap for excess target liquid keeps the pressure in the chamber to typically 10^{-3} mbar. To generate the x-ray-emitting

^{a)} Author to whom correspondence should be addressed; electronic mail: oscar.hemberg@biox.kth.se

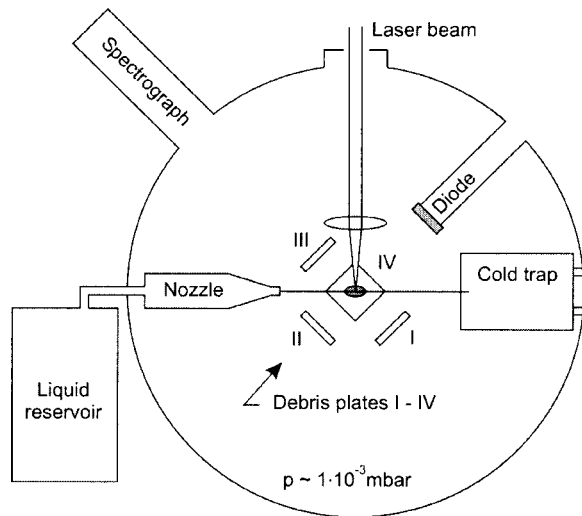


FIG. 1. Experimental arrangement.

plasma the beam from a 3 ns, $\lambda = 532$ nm 100 Hz Nd:YAG laser (Coherent Infinity) is focused with a 50 mm lens onto the liquid jet, typically 3–4 mm from the nozzle tip. The energy on target is ~ 65 mJ/pulse, which results in an intensity of $\sim 2 \times 10^{13}$ W/cm² given the full width half maximum (FWHM) of ~ 15 μ m in the focus. The laser plasma is optimized by adjusting the jet for maximum photon flux at the filtered x-ray diode (Hamamatsu G-1127-02). The diode is located at a $+45^\circ$ angle to the incident laser beam and outside the chamber, separated from the vacuum by a 350 nm Ti/200 nm Si₃N₄ filter and 6 mm of air. With this filter the x-ray signal is dominated by the $\lambda = 3.37$ nm C VI emission line, the line we presently use for our major application, microscopy.

III. DEBRIS MEASUREMENTS

In this section we discuss the procedure to measure debris and present experimentally determined debris deposition rates for ethanol and methanol. Finally, we speculate on the reason for the more than 1 order of magnitude lower debris deposition rates of methanol.

For characterization of the emitted debris, carefully cleaned glass microscope slides are positioned in the vacuum chamber approximately 25 mm from the plasma. Figure 1 shows the different positions (I–IV). Glass plate IV is placed below the plasma. On each slide a reference area is protected from the plasma by a small glass mask. The typical exposure times at continuous 100 Hz operations are 1 and 2 h for ethanol and methanol, respectively. For the 12 μ m methanol jet where the exposure time is 4 h, since the debris deposition rate is very low. The signal from the filtered x-ray diode is logged to ensure that for 95% of the pulses the x-ray flux is at least 80% of the maximum value. For both methanol and ethanol, the pulse-to-pulse fluctuations are typically 12% and the long-term drift is $\leq 2\%$.

For the thickness measurement of the deposited carbon debris layers we used the optical absorption method described in Ref. 6. We preferred the optical absorption measurements before profilometer measurements (cf. below)

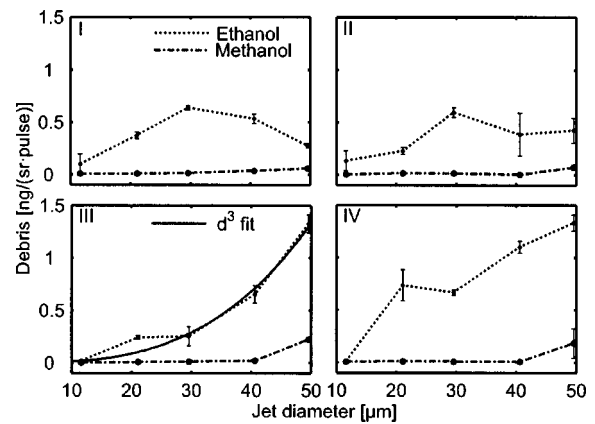


FIG. 2. Quantitative debris deposition for methanol and ethanol as function of the jet diameter for four different positions.

since the optical method has a high throughput and is sensitive (a minimum measurable thickness of 2 nm corresponds to an absorption difference of 0.5%). Furthermore, the method is especially advantageous when the edge between the protected and unprotected part is not sharp enough to provide distinct data from the profilometer. However, the optical method has to be used with care. Different plasma parameters (due to, e.g., a different laser pulse length) could change the optical absorption coefficient.^{18–20} Therefore a careful calibration for each laser–plasma experiment is always necessary.

The optical absorption method is calibrated with a profilometer (KLA-Tencor P15). We performed the calibration for three different experimental conditions: a 1 h exposure to a 22 μ m diam ethanol-jet plasma, a 1/2 h exposure to a 41 μ m ethanol-jet plasma, and a 2 h exposure to a 22 μ m methanol-jet plasma. The resulting profilometer measurements of thickness (110 ± 10 , 80 ± 10 , and 15 ± 10 nm, respectively) correspond to the following optical absorption coefficients: $(2.9 \pm 0.5) \times 10^4$, $(2.5 \pm 0.5) \times 10^4$, and $(3.2 \pm 2) \times 10^4$ cm⁻¹, respectively. The last optical absorption coefficient has a large uncertainty, since the measured debris layer thickness is in the same order as the surface roughness of the substrate (~ 5 nm). Combining the three measurements results in an optical absorption coefficient of $(3 \pm 0.5 \times 10^4)$ cm⁻¹. This value is well within the range of optical absorption coefficient found in literature for hydrogenated amorphous carbon (between 10^2 and 10^5 cm⁻¹).^{18–20} The large variation in the optical absorption coefficient discussed in the literature is caused by the dependence of the absorption coefficient on the ratio of sp^2 and sp^3 bonds in the amorphous carbon. This ratio is strongly dependent on the deposition conditions.

The results of the debris measurements as a function of the jet diameter are depicted in Fig. 2 for the four different positions I, II, III and IV (cf. Fig. 1). The error bars are determined by calculating the standard deviation of the debris thickness for five random measurement points on the debris plate. Typically the standard deviation is around 20% of the average debris thickness. This deviation is caused by the variation of the debris deposition. In addition, the debris deposition varies systematically so that it has a maximum in

the plane of the jet and the incoming laser beam and decreases further away from this plane.

As can be seen from Fig. 2, the debris deposition for ethanol at positions I and II (behind the jet) decrease for large jet diameters. This effect is probably due to shielding of ionic debris by the jet itself since the large-diameter jets constitute a thick target. Given the relatively low pulse energy and that the focus size is smaller than the jet, the back part of the plasma and the wings will consist of comparatively cold and dense target material that may block most of the high-energy carbon debris ions. For position III, a fit to $\sim d^3$, where d is the jet diameter, is inserted. In principle this behavior should occur in all four directions (since d^3 in the first approximation is proportional to the heated target mass) but, as stated above, we believe the debris in other directions is reduced by shielding by cold parts of the jet.

The most surprising observation in Fig. 2 is the 1 order of magnitude difference between the effective debris deposition rate for methanol and ethanol. Based on the carbon content, methanol should only result in a 37% reduction of debris. For example, in position III, the debris deposition from a 40 μm methanol jet is 20 ± 10 pg/(sr pulse) compared to 650 ± 150 pg/(sr pulse) for a 40 μm ethanol jet and 21 ± 10 pg/(sr pulse) for a 10 μm ethanol jet. Position III is of special interest since this is the direction of multilayer condenser mirror in our current x-ray microscope.¹³ These data are somewhat higher than previous measurements⁶ but still within the error bars. Another important difference between methanol and ethanol is the deposition of large clusters. Inspection of the debris slides by optical microscopy and measurements in the profilometer reveal significant amounts of clusters (diameter typically 0.1–1 μm) for ethanol jet diameters larger than 20 μm diameter, while no clusters can be detected for the methanol target regardless of the jet diameter.

A plausible explanation for the large difference in debris could be reactive ion etching (RIE) by oxygen.²¹ Since the C/O ratio is 1 for methanol and 2 for ethanol, this process should be much more effective for methanol than for ethanol. Hydrogen etching is also well known but the C/H ratios differ only 20% between methanol and ethanol. Note that the typical plasma temperature of the source (on the order of 100 eV) is in the same range as the typical oxygen ion energy in an RIE dry etcher. To determine whether the properties of the emitted ions from the plasma are appropriate for oxygen etching, commercially available glass plates coated with 200 nm of carbon were placed at position II and III. Although the carbon on the glass plates is much softer (more graphite like) than the amorphous carbon on the debris plates, any reduction of the carbon layer thickness should still gives an indication of a possible mechanism.

After 1 h of continuous operation of a 21 μm methanol jet, the carbon layers in direction II and III are indeed reduced by 40 ± 10 and 100 ± 10 nm, respectively, which corresponds to etch rate between 150 and 400 pg/(sr pulse). The etch rate in direction III is strongly dependent on the angle with the incoming laser beam. The smaller the angle, the larger the etch rate: for an angle of 30° around 150 nm carbon is removed. This is in agreement with the debris mea-

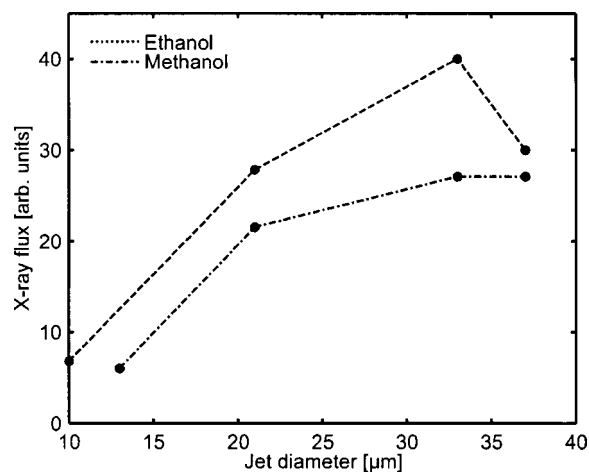


FIG. 3. Photon flux for the C VI $\lambda = 3.37$ nm line as function of the jet diameter for liquid methanol and ethanol jet target.

surements, the debris layer in direction III get thinner as the angle with the laser beam decreases.

These experiments show that oxygen (and possibly hydrogen) etching occur and that the lower debris deposition for the methanol target is probably due do a self-cleaning plasma. If only this process would be involved, the same results should be obtained with an ethanol/water mixture with a molar ratio of 1, since this mixture has a C/O ratio of 1 as well. For a 40 μm jet the debris in direction III is reduced according to the hypothesis [from 650 ± 150 to 30 ± 15 pg/(sr pulse)], while the debris in direction II remains the unchanged within the measurement accuracy [from 530 ± 150 to 710 ± 150 pg/(sr pulse)]. The reason for this is not clear to us. One may speculate that the properties of the ion emission from the plasma (e.g., lower temperature) is directionally nonuniform or that cluster formation is more important on the backside of the jet.

IV. PHOTON FLUX MEASUREMENTS

In this section we compare the $\lambda = 3.37$ nm x-ray flux of the methanol and ethanol as function of the jet diameter. Spectra at a -45° angle to the incident laser beam, are recorded with a 10 000 lines/mm free-standing transmission grating in combination with a cooled, thinned, back-illuminated 1024×1024 pixel charge coupled device array (SI003B).²² To suppress the scattered green light a filter is placed in front of the grating (200 nm Al combined with 450 nm of cellulose nitrate). The relative flux of the $\lambda = 3.37$ nm C VI line was determined for a range of jet diameters, from 10 to 40 μm , by integrating over the full line ($>10\%$ of peak intensity).

The results of the flux measurements are shown in Fig. 3. The measurements are taken in direction III to be comparable with the discussion of the debris deposition. Note the saturation at larger jet diameters due to the limited laser pulse energy. The x-ray flux for methanol is on average approximately 40% lower than the flux from ethanol. This is in accordance with the carbon content, which is 37% lower (by volume) in methanol compared to ethanol. No effort was made to perform accurately calibrated quantitative flux mea-

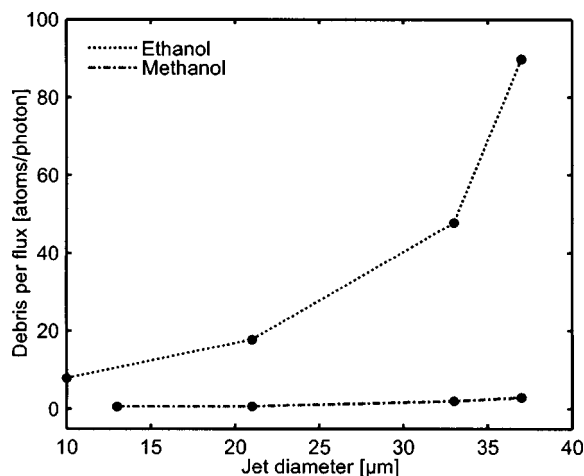


FIG. 4. Debris divided by photon flux for the $C\text{ VI } \lambda = 3.37\text{ nm}$ line expressed in numbers of debris atoms per emitted photon.

measurements since the scope of the present article is on the relative differences between ethanol and methanol. However, it should be noted that a rough estimate of the absolute photon flux [maximum: $4 \times 10^{11}\text{ ph}/(\text{sr} \times \text{pulse} \times \text{line})$] can be made provided one accepts a large accumulated calibration error (\sim factor of 2). This number is consistent with previous quantitative data,²² when taking the different laser energy and pulse width of the present experiment into account.

V. DISCUSSION AND CONCLUSIONS

When the liquid-jet laser-plasma source is operated in an application, e.g., an x-ray microscope, the deposited debris per exposure is more important than absolute debris deposition number discussed in Sec. III. In most applications a fixed number of photons are required for a good exposure and the debris-induced damage to optics is therefore linear to the number of exposures. Damaging debris deposition between exposures can mostly be avoided by shutters. To get a fair comparison of the applicability of the two sources, the debris per flux is chosen as a figure of merit and plotted in Fig. 4 for direction III. Here the flux data from Fig. 3 and the debris data of Fig. 2 are combined by interpolation of the debris values. The debris is expressed in number of atoms per photon, where the error is estimated to be a factor of 3.

It can be concluded from Fig. 4 that methanol is superior to ethanol as a target material: the debris per photon is one order of magnitude less than for ethanol. Although we do not fully understand the mechanism of debris reduction, our investigations clearly indicate that reactive oxygen etching is a plausible mechanism and the main reason for the large difference. In addition we have shown that cluster debris is significantly reduced with methanol. Although more experiments have to be performed, the most important conclusions are the existence of processes that can strongly reduce deposition and that the effective debris deposition can be strongly dependent on the target material. This knowledge could, e.g., also be of use to reduce debris of tape targets.

From Fig. 4 it may also be concluded that smaller jet diameters, in principle, are preferable. This is in accordance

with previous results. However, larger-diameter-jet plasmas make the illumination less sensitive to thermal drifts. Thus, larger jets giving shorter exposure times with a slightly higher debris deposition may be preferred when operating applications. Furthermore, we have previously deemed the debris deposition from a $10\text{ }\mu\text{m}$ ethanol jet to be acceptable in our current x-ray microscope, therefore methanol jets up to $40\text{ }\mu\text{m}$ could be used. This would reduce the debris a factor of 2 and increase the photon flux a factor of 3 compared to the current situation.

In applications where imaging optics are used as condensers, optical brightness is of greater importance than absolute photon numbers for reducing exposure times. This is, e.g., the case for microscopy. However, measurements on 11, 14, and $20\text{ }\mu\text{m}$ jets show a constant source diameter (within 10% FWHM) independent of jet diameter. This is supported by previous measurements with the same laser type on larger jets and other target materials.^{23,12,24} These results indicate that the optical brightness will scale almost linearly with the absolute photon flux. Given the results in Fig. 3 this would mean the exposure times could indeed be reduced by operation with methanol instead of ethanol also for these applications.

In summary, we have shown that methanol is preferred over ethanol as target liquid for carbonous liquid-jet target laser plasmas since the effective debris deposition rate is significantly reduced. Although the x-ray flux is somewhat lower for similar jet diameters, the large difference in debris allows the use of larger diameter jets, providing an increase in the x-ray flux. Since the plasma size hardly increases with jet diameter, the optical brightness should increase at the same rate as the photon flux. This could lead to either a longer lifetime of the x-ray optics or to a reduction in exposure times when using liquid-jet laser plasmas as sources for applications.

ACKNOWLEDGMENTS

The authors thank U. Vogt, R. Fruke, H. Stollberg, and P. Jansson for the size measurements, and gratefully acknowledge Göran Johansson and the financial support from the Swedish Science Research Council and the Wallenberg Foundation.

¹T. Mochizuki, T. Yabe, K. Okada, M. Hamada, N. Ikeda, S. Kiyokawa, and C. Yamanaka, *Phys. Rev. A* **33**, 525 (1986).

²L. Rymell and H. M. Hertz, *Opt. Commun.* **103**, 105 (1993).

³L. Rymell, M. Berglund, and H. M. Hertz, *Appl. Phys. Lett.* **66**, 2625 (1995).

⁴L. Malmqvist, L. Rymell, M. Berglund, and H. M. Hertz, *Rev. Sci. Instrum.* **67**, 4150 (1996).

⁵M. Berglund, L. Rymell, T. Wilhein, and H. M. Hertz, *Rev. Sci. Instrum.* **69**, 2361 (1998).

⁶L. Rymell, M. Berglund, and H. M. Hertz, *Rev. Sci. Instrum.* **66**, 2625 (1995).

⁷B. A. M. Hansson, L. Rymell, M. Berglund, and H. M. Hertz, *Microelectron. Eng.* **53**, 667 (2000).

⁸H. M. Hertz, L. Rymell, M. Berglund, and L. Malmqvist, *Proc. SPIE* **2523**, 88 (1995).

⁹U. Vogt, H. Stiel, I. Will, P. V. Nickles, W. Sandner, M. Wieland, and T. Wilhein, *Appl. Phys. Lett.* **79**, 2336 (2001).

¹⁰M. Wieland, T. Wilhein, M. Faubel, Ch. Ellert, M. Schmidt, and O. Sublemontier, *Appl. Phys. B: Lasers Opt.* **B72**, 591 (2001).

- ¹¹R. J. Tompkins *et al.*, *Rev. Sci. Instrum.* **69**, 3113 (1998).
- ¹²M. Berglund, L. Rymell, M. Peuker, T. Wilhein, and H. M. Hertz, *J. Microsc.* **197**, 268 (2000).
- ¹³G. A. Johansson, A. Holmberg, H. M. Hertz, and M. Berglund, *Rev. Sci. Instrum.* **73**, 1193 (2002).
- ¹⁴G. A. Johansson, M. Berglund, J. Birch, F. Eriksson, and H. M. Hertz, *Rev. Sci. Instrum.* **72**, 58 (2001).
- ¹⁵H. Kondo, T. Tomie, and H. Shimizu, *Appl. Phys. Lett.* **72**, 2668 (1998).
- ¹⁶O. Hemberg, B. A. M. Hansson, M. Berglund, and H. M. Hertz, *J. Appl. Phys.* **88**, 5421 (2000).
- ¹⁷J. de Groot, G. A. Johansson, and H. M. Hertz, *Rev. Sci. Instrum.* **74**, 3881 (2003).
- ¹⁸A. Helmbold and D. Meissner, *Thin Solid Films* **283**, 196 (1996).
- ¹⁹L. H. Chou and H. W. Wang, *J. Appl. Phys.* **74**, 4763 (1993).
- ²⁰Z. Y. Chen and J. P. Zhao, *J. Appl. Phys.* **87**, 4268 (2000).
- ²¹M. A. Lieberman and A. J. Lichtenberg, *Principles of Plasma Discharges and Materials Processing* (Wiley, New York, 1994).
- ²²T. Wilhein, S. Rehbein, D. Hambach, M. Berglund, L. Rymell, and H. M. Hertz, *Rev. Sci. Instrum.* **70**, 1694 (1999).
- ²³U. Vogt, M. Wieland, T. Wilhein, M. Beck, and H. Stiel, *Rev. Sci. Instrum.* **72**, 53 (2001).
- ²⁴M. Wieland, Master's thesis, Georg-August-Universität, Göttingen, Germany.